

# Magnon-magnon interactions in the Spin-Peierls compound

## $\text{CuGeO}_3$

Claudius Gros<sup>1</sup>, Wolfgang Wenzel<sup>1</sup>, Andreas Fledderjohann<sup>2</sup>

P. Lemmens<sup>3</sup>, M. Fischer<sup>3</sup>, G. Güntherodt<sup>3</sup>, M. Weiden<sup>4</sup>, C. Geibel<sup>4</sup>, F. Steglich<sup>4</sup>

<sup>1</sup> *Institut für Physik, Universität Dortmund, 44221 Dortmund, Germany*

<sup>2</sup> *Physics Department, University of Wuppertal, 42097 Wuppertal, Germany*

<sup>3</sup> *2. Physikalisches Institut, RWTH Aachen, 52056 Aachen, Germany*

<sup>4</sup> *FB Technische Physik, TH-Darmstadt, Hochschulstr. 8, 64289 Darmstadt, Germany*

(July 27, 2021)

## Abstract

In a magnetic substance the gap in the Raman spectrum,  $\Delta_R$ , and the neutron scattering gap,  $\Delta_S$ , are related by  $\Delta_R/\Delta_S \approx 2$  if the magnetic excitations (magnons) are only weakly interacting. But for  $\text{CuGeO}_3$  the experimentally observed ratio is of the order  $\Delta_R/\Delta_S \sim 1.49 - 1.78$ , indicating attractive magnon-magnon interactions in the quasi-1D Spin-Peierls compound  $\text{CuGeO}_3$ . We present numerical estimates of  $\Delta_R/\Delta_S$  from exact diagonalization studies for finite chains and find agreement with experiment for intermediate values of the frustration parameter  $\alpha$ . An analysis of the numerical Raman intensity leads us to postulate a *continuum* of two-magnon bound states in the Spin-Peierls phase. We discuss in detail the numerical method used, the dependence of the results on the model parameters and a novel matrix-element effect due to the dimerization of the Raman-operator in

the Spin-Peierls phase.

42.65.-k,78.20.-e,78.20.Ls

The Spin-Peierls compound  $\text{CuGeO}_3$  has lately been studied intensively [1] and found to exhibit well defined magnetic excitations (magnons) in the dimerized phase [2]. These magnons are found [3] to be separated by a gap from the continuum of two-spinon excitations predicted for the Heisenberg-chain [4] and were recently observed in  $\text{KCuF}_3$  [5] and in  $\text{CuGeO}_3$  [6]. In this context it was realized [7–9] that the magnons in the dimerized Heisenberg chain can be regarded as two-spinon bound-states. While spinons are essentially free in a homogeneous spin chain they interact strongly in a (gapped) dimerized spin chain where magnons are well defined excitations with dispersion  $\omega_q$  contributing a delta-function  $\sim \delta(\omega - \omega_q)$  to the dynamical structure factor,  $S(q, \omega)$ .

It is then all but natural to investigate the interactions of two magnons in a dimerized spin-chain. Here we will present numerical and experimental evidence that magnons do strongly interact in dimerized spin chains leading to a continuum of two-magnon bound states. For this purpose we will present data from exact diagonalization of chains with up to  $N_s = 28$  sites and experimental Raman spectra for  $\text{CuGeO}_3$ . We will, in particular, investigate the gap  $\Delta_S$  observed in  $S(q, \omega)$  and the gap  $\Delta_R$  observed in the two-magnon Raman spectrum  $I_R(\omega)$ . We find generally that  $\Delta_S/\Delta_R < 2$ , indicating strong magnon-magnon interactions in 1D dimerized spin systems.

As the minimal model for magnetic excitations in  $\text{CuGeO}_3$  one can consider the frustrated 1D spin Hamiltonian

$$H = J \sum_i [(1 + \delta(-1)^i) \mathbf{S}_i \cdot \mathbf{S}_{i+1} + \alpha \mathbf{S}_i \cdot \mathbf{S}_{i+2}] , \quad (1)$$

where  $\delta$  is the dimerization parameter that vanishes above  $T_{SP}$  [10,11]. The special geometry [12,13] of the superexchange path in  $\text{CuGeO}_3$  along the c-axis leads to a small value of the exchange integral  $J \approx 150\text{K}$  and a substantial n.n.n. frustration term  $\sim \alpha$  which competes with the n.n. antiferromagnetic exchange. The correct value of  $\alpha$  suitable for  $\text{CuGeO}_3$  is still under discussion. While Castilla *et al.* proposed  $\alpha \approx 0.24$  [10], a much larger value  $\alpha \approx 0.35$  was proposed by Riera and Dobry [11] and, recently, by Brenig *et al.* [14]. The interchain couplings have been estimated to be small,  $J_b \approx 0.1J$  and  $J_a \approx -0.01J$  for the

interchain exchange constants along a- and b- directions, respectively [2].

The phase diagram of  $H$  in Eq. (1) has been calculated using the density-matrix renormalization-group method [15]. For  $\delta = 0$  and  $\alpha < \alpha_c \approx 0.2411$ , the ground state is gapless and renormalizes to the Heisenberg fixed point. For  $\alpha = 0.5$  and  $\delta = 0$ , the ground state is given by a valence-bond state with a gap of order  $J/4$  induced by frustration.

An experimental method particularly suited for the study of magnetic excitations in an antiferromagnet is two-magnon Raman scattering. For  $\text{CuGeO}_3$ , the Raman operator in  $A_{1g}$  symmetry [16] is proportional [17] to

$$H_R = \sum_i (1 + \gamma(-1)^i) \mathbf{S}_i \cdot \mathbf{S}_{i+1} . \quad (2)$$

In the homogeneous state ( $\delta = \gamma = 0$ ) the Raman operator commutes with the Heisenberg Hamiltonian for the case  $\alpha = 0$  and there would be no Raman scattering [17,18]. However when  $\alpha \neq 0$ , the model (1) leads to magnetic Raman scattering  $\sim \alpha^2$  due to the presence of competing interactions which can be observed experimentally. Note the presence of the factor  $\gamma$  in Eq. (2) which appears for  $T < T_{SP}$  because the exchange integral is sensitive to the inter-ionic distance.

We have exactly diagonalized Eq. (1) for chains with up to 28 sites by a generalized Lanczos method and evaluated the Raman spectral weight at zero temperature,

$$I_R(\omega) = -\frac{1}{\pi} \text{Im} \langle 0 | H_R \frac{1}{\omega + i\epsilon - (H - E_0)} H_R | 0 \rangle, \quad (3)$$

where  $E_0$  is the ground state energy,  $H$  the Hamiltonian given by Eq. (1) and  $\epsilon \rightarrow 0+$ . We have also calculated the dynamical structure factor

$$S(q, \omega) = \sum_n |\langle n | S_q^z | 0 \rangle|^2 \delta(\omega - (E_n - E_0)) \quad (4)$$

where  $S_q^z = N_s^{-1/2} \sum_{l=1}^{N_s} \exp[iql] S_l^z$  and  $|n\rangle$ ,  $E_n$  are the Eigenstates and Eigenenergies of the spin chain, respectively.

We have evaluated  $S(q, \omega)$  for chains with up to  $N_s = 24$  sites using an approximate scheme for the determination of the low lying excitation energies  $E_n - E_0$  and the corresponding transition probabilities  $w_n(q) = |\langle n | S_q^z | 0 \rangle|^2$  [19]. Using a recursion algorithm a set

of orthogonal states is built starting with  $S_q^z|0\rangle$ . Coefficients occuring in this procedure form a tridiagonal matrix whose eigenvalues and eigenstates determine the excitation energies and transition probabilities [9,19].

For a numerical evaluation of Eq. (3), we have used the *kernel polynomial approximation*. Since the advantages of this method have been realized only recently [20] we give here a brief account. We start by rescaling the Hamiltonian by  $H = cX + d$  such that the eigenvalues of the rescaled Hamiltonian  $X$  are in the interval  $[-1, 1]$ . Similary we define a rescaled energy and frequency by  $E_0 = cx_0 + d$  and  $\omega = cx + d$  and expand  $I_R(x)$  in terms of Tschebycheff polynomials,  $T_l(x)$ :

$$I_R(x) = \frac{1}{\sqrt{1-x^2}} \sum_{l=0}^{N_p} a_l T_l(x + x_0), \quad (5)$$

where the number of polynomials retained,  $N_p$ , determines the accuracy of the approximation which becomes exact in the limit  $N_p \rightarrow \infty$ . The expansion coefficients  $a_l$  are determined using the orthogonality relations for Tschebeycheff polynomials to be

$$a_l = \frac{2 - \delta_{l,0}}{\pi} \langle 0 | H_R T_l(X) H_R | 0 \rangle,$$

which can be evaluated recursively via the formula  $T_{l+1}(x) = 2xT_l(x) - T_{l-1}(x)$ . The advantage of an expansion in orthogonal polynomials is its numerical stability. It is indeed possible to evaluate several thousands of  $a_l$  recursively without encountering numerical instabilities. Often we will use only a limited number  $N_p = 100$  for comparison with experimental data.

A truncated expansion in orthogonal polynomials will, in general, lead to unwelcome Gibbs oscillations for any finite  $N_p < \infty$ . These Gibbs oscillations have been studied carefully in the past [20] and can be suppressed efficiently and reliable by the replacement  $a_l \rightarrow a_l g(z_l)$  with  $g(z_l) = [\sin(\pi z_l)/(\pi z_l)]^3$  and  $z_l = l/(N_p + 1)$  [20]. Note that this replacement, which we use throughout this paper, still satisfies the correct limit  $N_p \rightarrow \infty$ .

A finite  $N_p < \infty$  in (5) does broaden the delta-poles in a finite system calculation. The dependence of  $I_R(\omega)$  on  $N_p$  is illustrated in Fig. 1 for a chain with  $N_s = 28$  sites,  $\alpha = 0.24$  and  $\delta = 0 = \gamma$ . In the inset of Fig. 1 we compare the broadening of a single pole with the kernel

polynomial approximation ( $N_p = 100$ ) with a Lorentzian  $\epsilon/((\omega - \omega_i)^2 + \epsilon^2)$  and  $\epsilon = 0.025$ . Note the absence of the high-energy tails in the kernel polynomial approximation.

We have measured the Raman intensity on single crystal  $\text{CuGeO}_3$  using the excitation line  $\lambda = 514.5\text{-nm}$  of an Ar-laser with a laser power of 2.7mW. We ensured that the incident radiation does not increase the temperature of the sample by more than 1.5 K. We used a DILOR-XY spectrometer and a nitrogen cooled CCD (back illuminated) as a detector in a quasi backscattering geometry with the polarization of incident and scattered light parallel to the c-axis and the Cu-O chains, respectively.

In Fig. 2, we present the data for the two-magnon Raman continuum in the homogeneous state at  $T = 20$  K. Phonon lines [22,23] at  $184\text{cm}^{-1}$  and at  $330\text{cm}^{-1}$  are subtracted from the experimental data (squares). The experimental Raman spectrum presented in Fig. 2 is in agreement with other Raman studies on  $\text{CuGeO}_3$  [22]. We have included in Fig. 2 the numerical results for  $I_R(\omega)$  obtained for chains with  $N_s = 24$  (dashed lines) and  $N_s = 28$  (solid lines) sites for  $\delta = 0 = \gamma$  and  $N_p = 100$ . Note that the finite-size effects are quite small. We show in Fig. 2 data for two parameter sets, namely  $\alpha = 0.24$ ,  $J = 150K$  and  $\alpha = 0.35$ ,  $J = 159K$ . We note that  $\alpha = 0.35$ , which is favoured by fits to the susceptibility [11] and to the specific heat [14] does not agree well with the Raman spectrum. Similar results have been obtained previously with a solitonic mean-field approach to the frustrated Heisenberg chain [17,24].

In the dimerized phase  $\delta \neq 0$  we have found that the numerically obtained Raman spectrum depends very much on the dimerization parameter  $\gamma$  in the Raman operator as we illustrate in Fig. 3 for a chain with  $N_s = 24$  sites,  $\delta = 0.03$ ,  $\alpha = 0.24$  and  $N_p = 100$ . Between  $\gamma = 0$  and  $\gamma = 0.15$  the spectrum changes qualitatively and a low-energy peak can be resolved for  $\gamma = 0.12, 0.15$ , but not for  $\gamma = 0$ .

In order to understand the dramatic dependence of the  $I_R(\omega)$  on  $\gamma$  observed in Fig. 3 we have analyzed the dependence of the seven lowest poles contributing to  $I_R(\omega)$  on  $\gamma$ , illustrated in the inset of Fig. 4 for  $N_s = 24$ ,  $\alpha = 0.24$ ,  $\delta = 0$ ,  $N_p = 1000$  and  $\gamma = 0$ .

We start by rewriting Eq. (3) in the form

$$I_R(\omega) = \sum_n |\langle 0|H_R|n\rangle|^2 \delta(\omega - (E_n - E_0)) \quad (6)$$

and noting that we can decompose the Raman operator into two parts,  $H_R = H' + \gamma H''$ .

The weight of an excited state then becomes

$$w_n = |\langle 0|H' + \gamma H''|n\rangle|^2 = |m' + \gamma m''|^2, \quad (7)$$

and for any  $n$  there is a  $\gamma_0 = -m'/m''$  for which  $w_n$  vanishes. We have analyzed the energy-dependence of  $\gamma_0 = \gamma_0(E_n)$  and found that for the five dominant poles,  $n = 1, 2, 4, 6, 7$

$$\gamma_0 \approx \delta + \frac{4}{3000} E_n, \quad (8)$$

in inverse wavelength [ $cm^{-1}$ ] for  $E_n$ . This dependence of  $w_n$  on  $E_n$  is shown in Fig. 4 where we have plotted the weights as a function of  $\gamma - \gamma_0(E_n)$ . The data presented in Fig. 4 clearly indicates that the dominant contributions to  $I_R(\omega)$  follow the scaling relation

$$\rho(\gamma, E_i) = \frac{I_{\gamma=0}}{I_\gamma} \left( \frac{\gamma - \gamma_0(E_i)}{\gamma_0(E_i)} \right)^2, \quad (9)$$

where  $I_\gamma$  is a normalization constant, which we have approximated by the constraint  $\int_0^{\omega_c} d\omega \rho(\gamma, \omega) = 1$ , with  $\omega_c = 6J$ . The scaling relation Eq. (9) constitutes, on the other hand, also the rescaling of the Raman intensity  $I_R(\omega) = I_R(\gamma, \omega)$  with  $\gamma$ , such that we can write

$$I_R(\gamma, \omega) \approx \rho(\gamma, \omega) I_R(0, \omega). \quad (10)$$

We see that the effect of  $\gamma$  is to “burn a spectral hole” in  $I_R(0, \omega)$  at a characteristic frequency  $\gamma_0(\omega)$ , in agreement with the numerical results presented in Fig. 3.

We can actually find a complete analytic formula for  $I_R(\gamma, \omega)$  by noting that for  $\alpha = 0.24$ ,  $\delta = 0.03$  we can approximate  $I_R(0, \omega)$  by the expression (see Fig. 3 and [17])

$$I_R(\gamma = 0, \omega) = A \theta(\omega - \Delta_R) (1 - \tanh[2(\omega - \omega_0)]), \quad (11)$$

with the values of the parameters  $\Delta_R \approx 30 cm^{-1}$ ,  $\omega_0 \approx 312 cm^{-1}$  being determined by a fit to the numerical data ( $A$  is a normalization constant). The heavy-side function  $\theta(\omega - \Delta_R)$  in Eq. (11) reflects the absence of two-magnon excitations below  $\Delta_R$  in the dimerized state.

In Fig. 5, we present the experimental Raman spectrum in the spin-Peierls phase at  $T = 5\text{K}$  (with phonon lines subtracted, filled squares) in comparison with the analytic result for  $\gamma = 0.12$  (Eq. (10) together with Eq. (11), solid line). Experimentally a two-magnon peak is observed at  $30\text{cm}^{-1}$  and a broad continuum at higher frequencies. These two features are well reproduced by the analytic result. There is, on the other hand, a new, probably magnetic line at  $225\text{cm}^{-1}$ , which is not reproduced by our theoretical study of the one-dimensional spin model (1), compare also Fig. 3. This fact has led us to speculate [17] that the interchain coupling  $J_B$  might become relevant for  $T < T_{SP}$  in  $\text{CuGeO}_3$ .

Which is the physical significance of the peak at  $\Delta_R \sim 30\text{cm}^{-1}$  in Fig. 5 observed both in experiment and in our analytical result? Neutron-scattering experiments [2,25] indicate a one-magnon gap  $\Delta_S \sim (2.1 - 2.5)\text{meV}$ , i.e.  $\Delta_S \sim (16.9 - 20.2)\text{cm}^{-1}$ . The experimental ratio

$$\left. \frac{\Delta_R}{\Delta_S} \right|_{\text{Exp.}} \sim 1.49 - 1.78 \quad (12)$$

is smaller than two, the value expected for non-interacting magnons. This indicates an attractive interaction between magnons in 1D dimerized spin chains, similar to the attraction between spinons. Uhrig and Schulz [8] have indeed postulated an isolated singlet bound state with energy  $E_s$  and  $2\Delta_S > E_s > \Delta_S$  which might be a two-magnon bound state.

A singlet bound-state with zero total momentum would be observable by Raman scattering and would show up as a delta-function contribution to the Raman intensity (6):

$$I_R(\omega) = A\delta(\omega - E_s) + I'_R(\omega),$$

with  $I'_R(\omega)$  being the continuum part of the Raman intensity. A finite weight  $A$  implies also a finite value of the relative weight of the first pole,

$$A_r = \lim_{N_s \rightarrow \infty} \frac{w_1}{\sum_n w_n}, \quad (13)$$

with  $w_n = |\langle 0 | H_R | n \rangle|^2$ . In the inset of Fig. 5 we show the relative weight as a function of  $1/N_s^2$  for chains with up to  $N_s = 28$  sites and  $\alpha = 0.24$ . We find no indication for an isolated



bound state, i.e. for a finite value of  $A_r$  both for  $\delta = 0$  (filled circles), as expected, and for  $\delta = 0.03$  (filled triangles). The data for  $\delta = 0.03$  shown in the inset of Fig. 5 have been calculated for  $\gamma = 0.12$ . The data for  $\gamma = 0$  and  $\delta = 0.03$  are very similar.

We have therefore no indication from numerics for an isolated singlet bound state, in agreement with our interpretation of the  $30\text{cm}^{-1}$  peak as a continuum contribution truncated by matrix-element effect, see Eq. (10). Our numerical results show, on the other hand, unambiguously that the lower edge of the Raman spectrum is pulled below the non-interacting two-magnon density of states. This fact, which is discussed in detail further below, indicates a *continuum* of two-magnon bound states with zero total momentum. This scenario is conceivable in view of the fact, that the two-magnon spectrum is made up out of four spinons

The experimentally observed values of single- and two-magnon gap energies can be used, to a certain extent, to determine the value of the parameters  $J$ ,  $\delta$  and  $\alpha$  entering Eq. (1). The ratio  $\Delta_R/\Delta_S$  is independent of the coupling-constant  $J$ . We have plotted  $\Delta_R/\Delta_S$  in Fig. 6 for various values of  $\alpha$  as a function of  $\delta$ . The data are obtained for  $N_s = 24$ , the finite-size corrections are very small (compare also [9]). The experimental possible values 1.49-1.78 are indicated as the shaded region in Fig. 6. Again, we see that a larger value of  $\alpha \sim 0.35$  does not do a good job on  $\Delta_R/\Delta_S$ . In using Fig. 6 for determining possible combinations of  $\alpha$  and  $\delta$  one has to keep in mind that the interchain coupling  $J_b$ , not included in our calculations, has an effect of order 10% on the values quoted in Fig. 6. It is interesting to note, that recent experiments on  $\text{CuGeO}_3$  under pressure [26] show that the frustration parameter  $\alpha$  increases with pressure, as does the experimental ratio  $\Delta_R/\Delta_S$ , in accordance with the data presented in Fig. 6.

In conclusion we have discussed in detail the effect of the dimerization of the Raman operator on the Raman spectrum in the spin-Peierls state of  $\text{CuGeO}_3$ . We have not found any numerical evidence for a singlet bound-state and conclude that the  $30\text{cm}^{-1}$  Raman line observed at  $T = 5\text{K}$  in  $\text{CuGeO}_3$  is a two-magnon line which is carved out of a continuum by matrix-element effects due to the dimerization of the Raman operator,  $\gamma$ . We have then

compared the observed ratio of the Raman gap to the neutron-scattering gap and compared with numerical results. We conclude that this ratio indicates an intermediate value for the frustration parameter  $\alpha$ .

## ACKNOWLEDGMENTS

This work was supported through the Deutsche Forschungsgemeinschaft, the Graduiertenkolleg “Festkörperspektroskopie”, SFB 341 and SFB 252, and by the BMBF 13N6586/8,

## REFERENCES

- [1] M. Hase, I Terasaki and K. Uchinokura, Phys. Rev. Lett. **70**, 3651 (1993).
- [2] M. Nishi, O. Fujita and J. Akimitsu, Phys. Rev. B **50**, 6508 (1994).
- [3] M. Aïn, J.E. Lorenzo, L.P. Regnault, G. Dhalenne, A. Revcolevschi and Th. Jolicoeur, “*Double gap and solitonic excitations in the spin-Peierls chain  $\text{CuGeO}_3$* ”, preprint.
- [4] See, e.g. G. Müller, H. Thomas, H. Beck and J.C. Bonner, Phys. Rev. B **24**, 1429 (1981).
- [5] D.A. Tennant, R.A. Cowley, S.E. Nagler and A.M. Tsvelik, Phys. Rev. B **52**, 13 368 (1995).
- [6] M. Arai *et al.*, Phys. Rev. Lett. **77**, 3649 (1996).
- [7] A.M. Tsvelik, Phys. Rev. B **45**, 486 (1992).
- [8] G.S. Uhrig and H.J. Schulz, Phys. Rev. B **54**, R9624 (1996).
- [9] A. Fledderjohann and C. Gros, “*Spin dynamics of dimerized Heisenberg chains*”, Euro. Phys. Lett., (in press, Sissa preprint cond-mat/9612013)
- [10] G. Castilla, S. Chakravarty and V.J. Emery, Phys. Rev. Lett. **75**, 1823 (1995).
- [11] J. Riera and A. Dobry, Phys. Rev. B **51**, 16 098 (1995); The authors estimate a slightly larger value of  $\alpha \approx 0.36$  than Castilla *et al.* [10].
- [12] M. Braden, G. Wilkenorf, J. Lorenzana, M. Aïn, G.J. McIntyre, M. Behruzi, G. Heeger, G. Dhalenn and A. Revcolevschi, Phys. Rev. B **54**, 1105 (1996).
- [13] D. Khomskii, W. Geertsma and M. Mostovoy, Sissa preprint cond-mat # 9609244.
- [14] W. Brenig *et al.*, personal communication.
- [15] R. Chitra *et al.*, Phys. Rev. B **52**, 6581 (1995).
- [16] P.A. Fleury and R. Loudon, Phys. Rev. **166**, 514 (1967).

- [17] V.N. Muthukumar, C. Gros, W. Wenzel, R. Valentí, P. Lemmens, B. Eisener, G. Güntherodt, M. Weiden, C. Geibel and F. Steglich, Phys. Rev. B **54**, R9635 (1996).
- [18] R.R.P. Singh, P. Prelovšek and B.S. Shastry, Phys. Rev. Lett. **77**, 4086 (1996).
- [19] A. Fledderjohann, M. Karbach, K.-H. Mütter and P. Wielath, J. Phys.: Condens. Matter **7**, 8993 (1995); V.S. Viswanath, S. Zhang, J. Stolze and G. Müller, Phys. Rev. B **49**, 9702 (1994).
- [20] R.N. Silver and H. Röder, Int. J. Mod. Phys. C **5**, 735 (1994); R.N. Silver, H. Röder, A.F. Voter and J.D. Kress, J. Comp. Phys. , in press.
- [21] P. Lemmens, M. Udagawa, M. Fischer, G. Güntherodt, M. Weiden, W. Richter, C. Geibel and F. Steglich, J. Phys. **46**, 1979 (1996).
- [22] H. Kuroe *et al.*, Phys. Rev. B **50**, 16 468 (1994); P.H.M. van Loosdrecht *et al.*, Phys. Rev. Lett. **76**, 311 (1996).
- [23] P. Lemmens, B. Eisener, M. Brinkmann, L.V. Gasparov, P.v. Dongen, M. Weiden, W. Richter, C. Geibel and F. Steglich, Physica B **223&224**, 535 (1996).
- [24] V.N. Muthukumar, C. Gros, R. Valentí, M. Weiden, C. Geibel, F. Steglich, P. Lemmens, M. Fischer and G. Güntherodt, “*The  $J_1 - J_2$  model revisited: Phenomenology of  $\text{CuGeO}_3$* ”, Phys. Rev. B (in press).
- [25] M.C. Martin, G. Shirane, Y. Fujii, M. Nishi, O. Fujita, J. Akimitsu, M. Hase and K. Uchinokura, Phys. Rev. B **53**, R14 713 (1996).
- [26] P. van Loosdrecht, private communication.

## FIGURES

FIG. 1. Dependence of the spectrum obtained by the kernel polynomial approximation on the number of Tschebyscheff polynomials,  $N_p = 100, 300, 800$ , retained. The data is for a chain with  $N_s = 28$  sites and  $\delta = 0 = \gamma$ ,  $\alpha = 24$ . For  $N_p \rightarrow \infty$  the poles evolve into delta-functions. Insert: Comparison between a pole located at  $x = 0.5$  broadened by a Lorentzian  $\epsilon/((x - 0.5)^2 + \epsilon^2)$  (dashed line), with  $\epsilon = 0.025$  and an orthogonal polynomial approximation with  $N_p = 100$  Tschebyscheff polynomials.

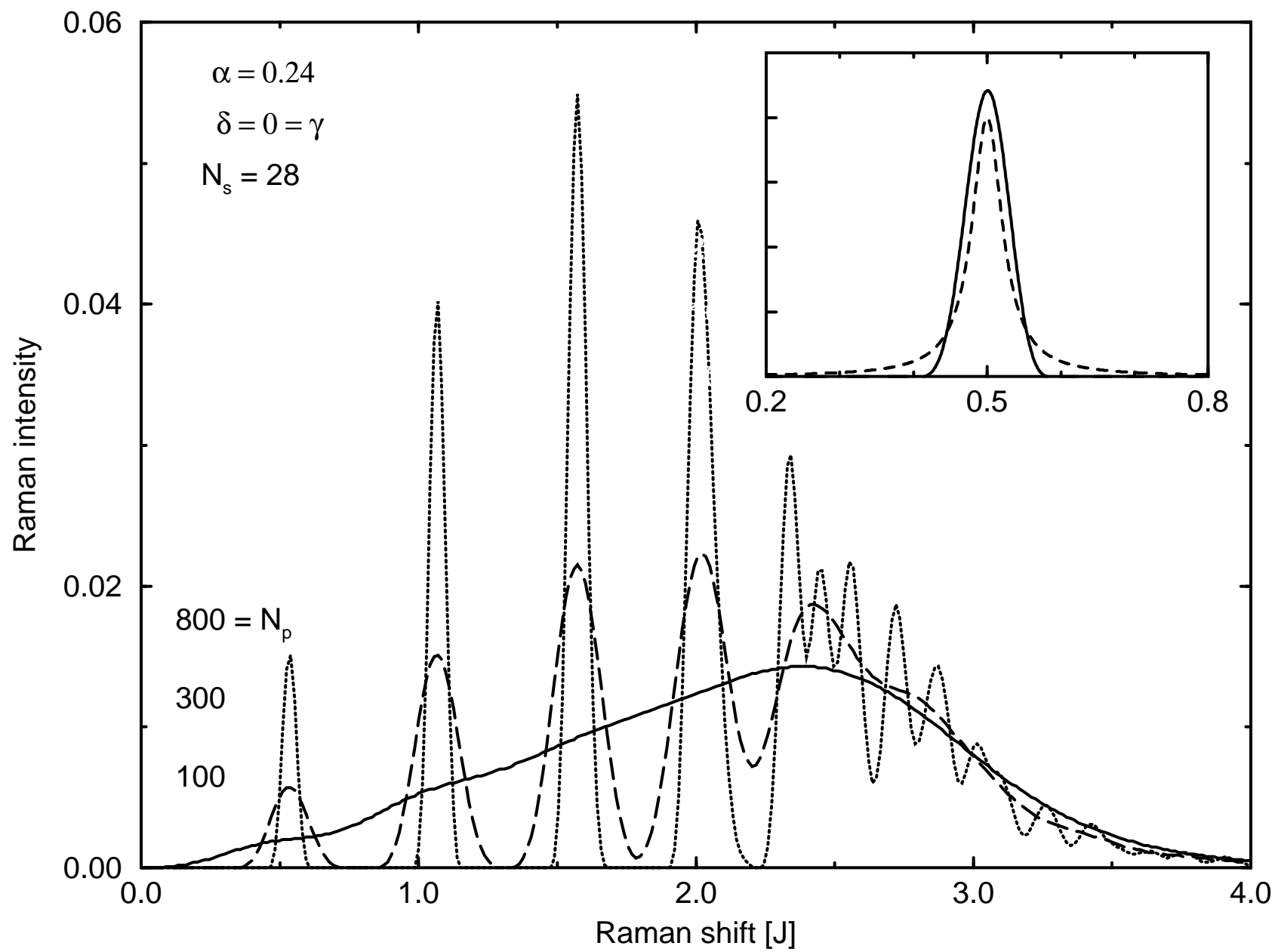
FIG. 2. The magnetic contribution to the experimental Raman spectrum for  $\text{CuGeO}_3$  at  $T = 20K$  (filled squares) and data obtained for chains with  $N_s = 24, 28$  sites (dashed/solid line) for  $\alpha = 0.24$  and  $\alpha = 0.35$  respectively and  $N_p = 100$  and  $\delta = 0 = \gamma$ .

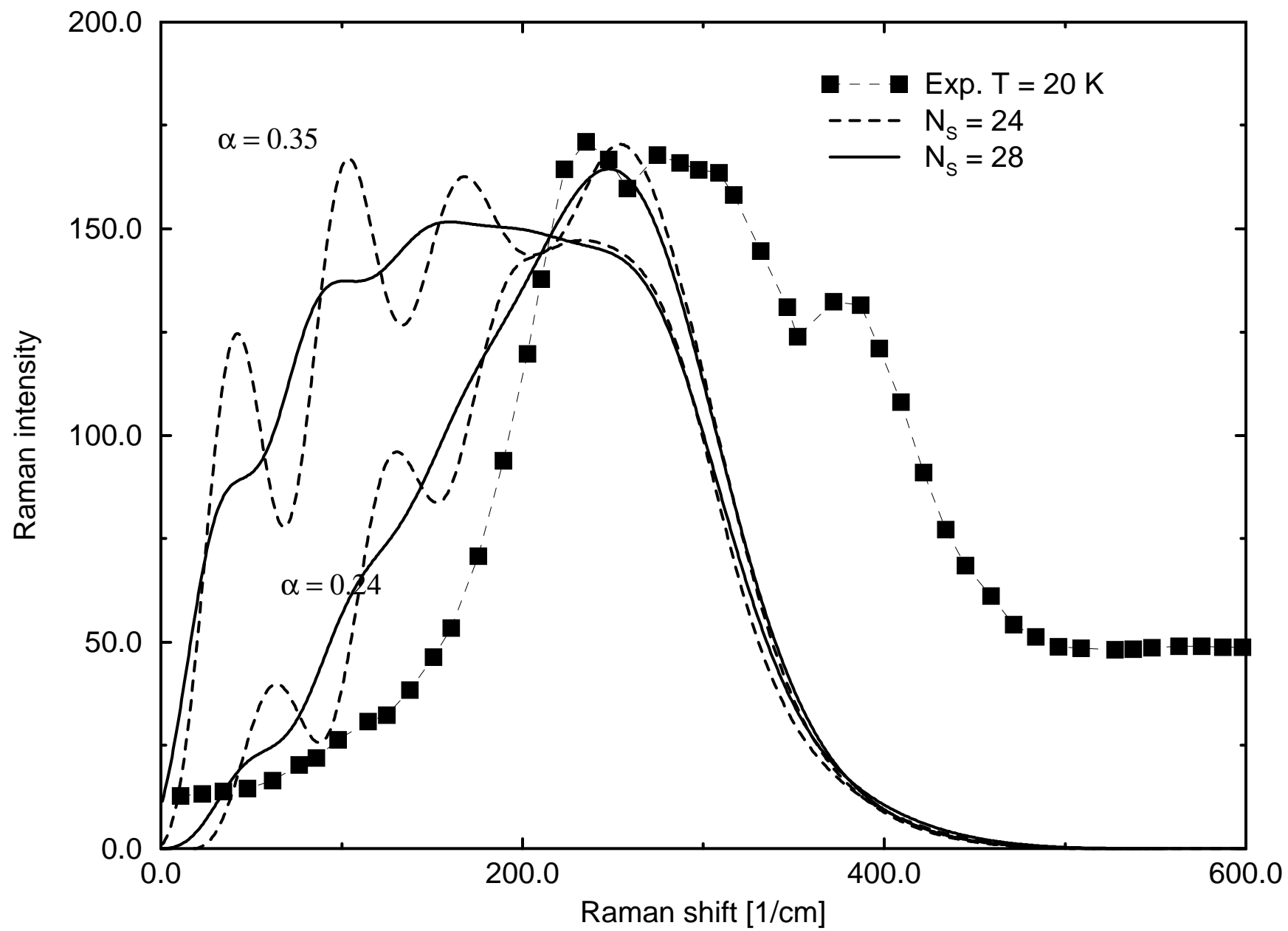
FIG. 3. Dependence of the spectrum in the dimerized phase,  $\delta = 0.03$ ,  $\alpha = 0.24$ ,  $N_p = 100$  for a chain with  $N_s = 24$  sites on the dimerization of the Raman-operator,  $\gamma = 0, 0.03, 0.06, 0.09, 0.12, 0.15$ . Note the large matrix-element effects.

FIG. 4. The rescaled weight  $w(E_n)$  of the lowest seven poles in the Raman spectrum with pole Energy,  $E_n$  ( $n = 1, \dots, 7$ ) as a function of the rescaled dimerization of the Raman operator,  $\gamma - \gamma_0(E_n)$ , see Eq. (8). The data is for a chain with  $N_s = 24$  sites and  $\delta = 0.03$ ,  $\alpha = 0.24$ . The weight is rescaled by  $\gamma_0(E_i) = \delta + \kappa E_i$ , with  $\kappa \approx 4/3000\text{cm}$ . We observed that the rescaled weights of the dominant poles 1, 2, 4, 6, 7 fall all on a universal curve (the data for pole number 4 has been omitted in order to avoid overcrowding).

FIG. 5. Comparison between the experimental Raman spectrum in the dimerized phase of  $\text{CuGeO}_3$  at  $T = 5K$  (filled squares) and the analytic expression ((10), solid line) Insert: The relative weight (Eq. (13)) of the lowest pole contribution to  $I_R(\omega)$  as a function of  $1/N_s^2$  for  $N_s = 12, 16, 20, 24, 28$ . The data is for  $\alpha = 0.24$ ,  $\delta = 0$  (filled circles) and  $\delta = 0.03$  and  $\gamma = 0.12$  (filled triangles).

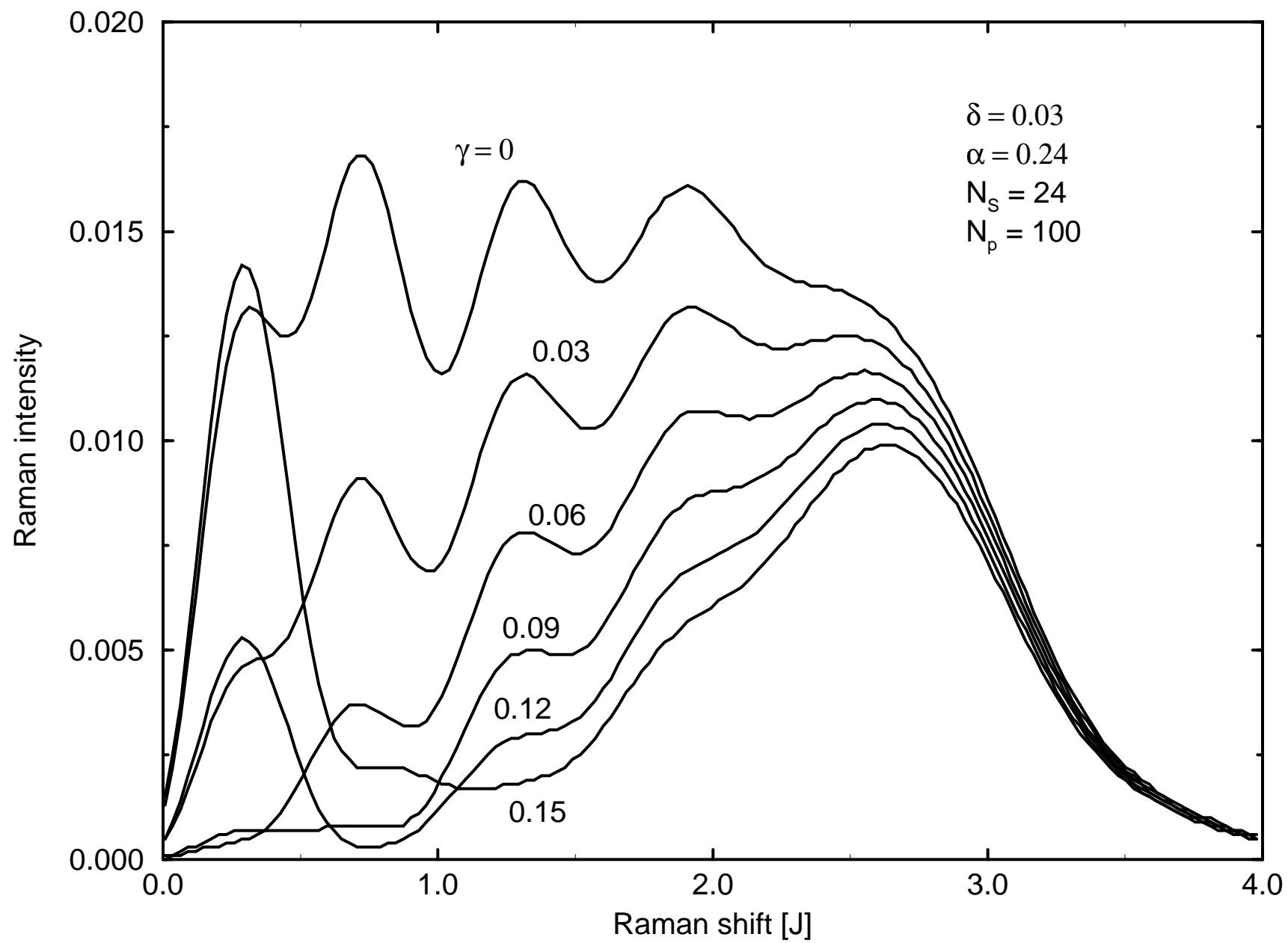
FIG. 6. The calculated ratios of the  $\Delta_R/\Delta_S$  from chains with  $N_s = 24$  sites for various  $\alpha$  and  $\delta$ . The shaded region indicates the experimentally observed values for  $\text{CuGeO}_3$ .

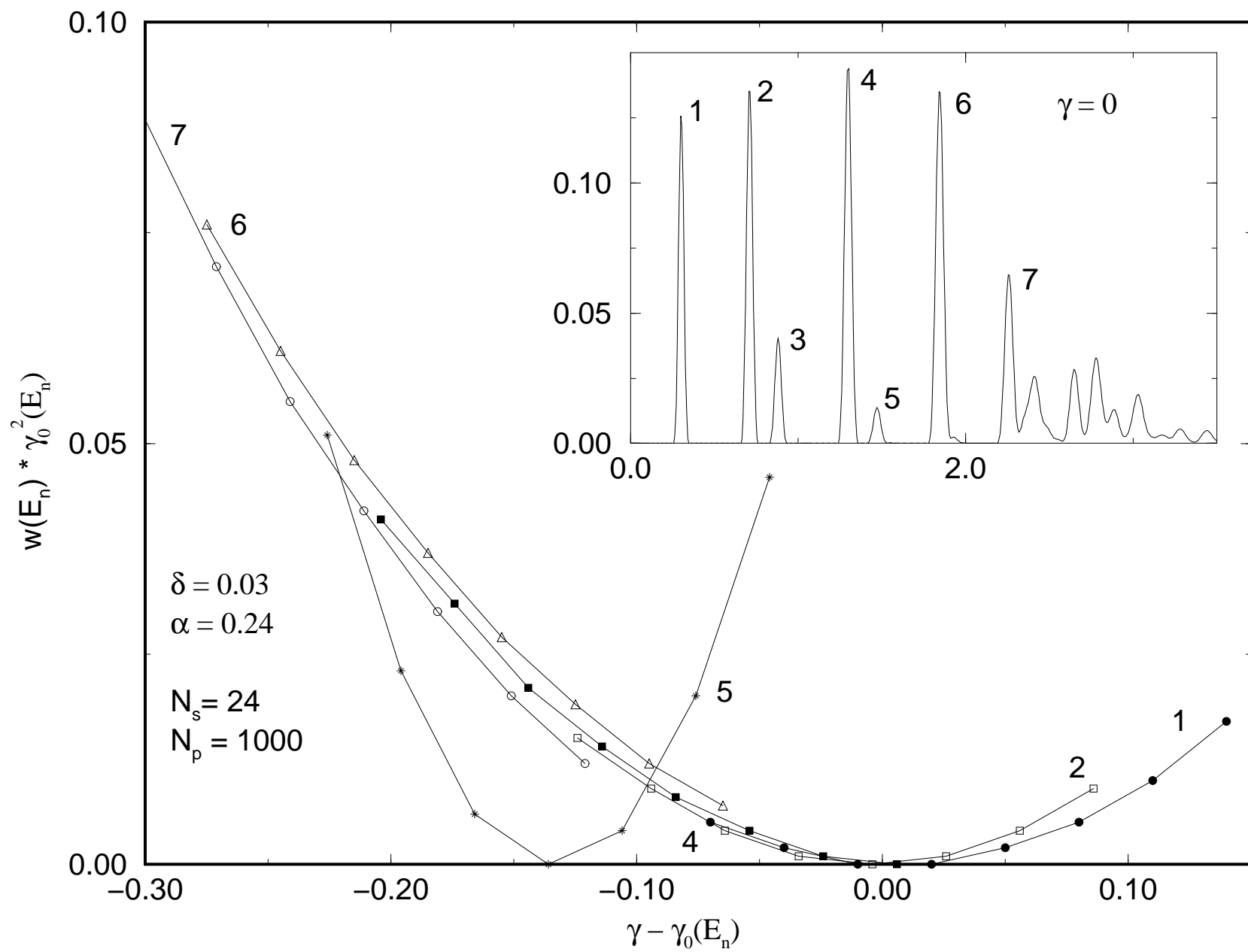


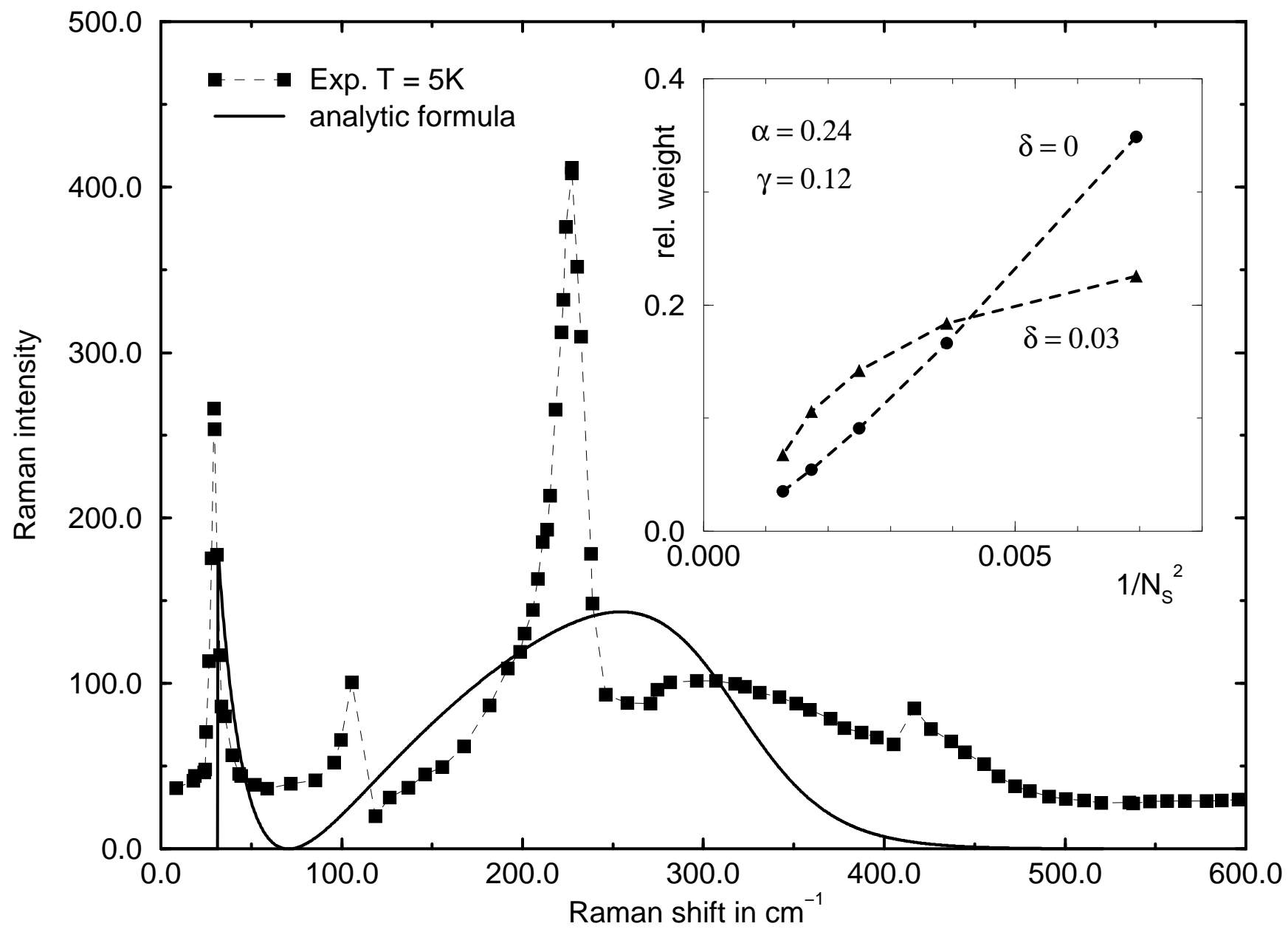


Gros et al. Fig. 2









Gros et al. Fig. 5

